Approximate theory of temperature coefficient of resistivity of amorphous semiconductors

Ming-Liang Zhang and D. A. Drabold

Phys. Rev. B **85**, 125135 — Published 29 March 2012

DOI: 10.1103/PhysRevB.85.125135

Approximate Theory of Temperature Coefficient of Resistivity of Amorphous Semiconductors

Ming-Liang Zhang and D. A. Drabold
Department of Physics and Astronomy, Ohio University, Athens, Ohio 45701

In this paper, we develop an approximate theory of the temperature coefficient of resistivity (TCR) and conductivity based upon the recently proposed Microscopic Response Method. By introducing suitable approximations for the lattice dynamics, localized and extended electronic states, we produce new explicit forms for the conductivity and TCR, which depend on easily accessible material parameters. The theory is in reasonable agreement with experiments on a-Si:H and a-Ge:H. A long-standing puzzle, a "kink" in the experimental $\log_{10}\sigma$ vs. 1/T curve, is predicted by the theory and attributed to localized to extended transitions, which have not been properly handled in earlier theories.

PACS numbers: 71.23.An, 71.38.Fp, 71.38.Ht.
Keywords: eigenvector of normal modes, conductivity, atomic displacement

I. INTRODUCTION

The temperature coefficient of resistivity (TCR) of an amorphous semiconductor (AS) is not only an important quantity in transport theory, but also a critical parameter controlling the sensitivity of uncooled microbolometers employed in thermal imaging "night vision" applications[1,2].

The conventional approach to transport coefficients is the kinetic method (Boltzmann or master equations etc.). However, this is not applicable even to crystalline semi-metals and semiconductors (the so-called Landau-Peierls criterion)[3–5]. Comparing to metals, the low carrier concentration in these materials results in a lower kinetic energy of carriers. Thus neither the elastic scattering by disorder, nor the inelastic scattering by a phonon has a well-defined transition probability per unit time[3–5]. In AS, the strong electron-phonon interaction of localized states requires a reorganization of the vibrational configuration for any transition involving localized state(s)[6,7]. For these intrinsic multi-phonon transitions, the energy conservation between initial and final electronic states (a basic condition of Fermi's golden rule)[3–5], is violated more seriously than that for single-phonon emission and absorption.

In addition, transitions between localized and extended states (LE and EL) are not treated adequately in a kinetic approach. The Miller-Abrahams theory[8] and its extensions suppose that LE and EL transitions do not directly contribute to conduction, and only maintain the distribution of carriers between localized states and extended states in thermal equilibrium (when an external electric field is absent) or in the non-equilibrium stationary state (when an external field is present). Electrical conduction is fulfilled by the transition from a localized state to another localized state (LL) and the transition from an extended state to another extended state (EE)[1,2,9]. The theory of phonon-induced delocalization and the theory of transient current excited by photon have heuristically estimated conductivity from LE and El transitions.

Rigorous expressions for the conductivity and Hall mobility in AS have been obtained in the microscopic response method (MRM)[7,10]. These expressions require transition amplitudes rather than transition probability per unit time[11]. Thus the long-time limit required in a kinetic approach[3,4] is avoided. To the lowest order self-consistent approximation, there are 29 processes contributing to conductivity and 10 processes contributing to Hall mobility[7]. For example, in a n-doped AS the conductivity from LE transitions driven solely by an external field is[7]

$$\left\{ \begin{array}{l} \mathrm{Re} \\ \mathrm{Im} \end{array} \right. \sigma_{\alpha\beta}(\omega) = -\frac{N_e e^2}{2\Omega_{\mathbf{s}}} \sum_{AB} \mathrm{Im} \frac{(w^{\alpha}_{AB} - v^{\alpha}_{BA})(v^{\beta}_{BA})^*}{(E^0_A - E^0_B)}$$

$$\times i[I_{BA+} \pm I_{BA-}][1 - f(E^0_B)]f(E^0_A), \quad \alpha,\beta = x,y,z, \quad (1)$$

where the real part takes the upper sign, imaginary part the lower sign. $\Omega_{\mathbf{s}}$ is the physical infinitesimal volume element used to take spatial average. An AS can be viewed as uniform when we measure its properties (e.g. conductivity) at a linear length scale larger than[12] 10nm. If we take $\Omega_{\mathbf{s}}$ as a sphere with a radius larger than 5nm, then the choice of the center $\mathbf{s}$ of $\Omega_{\mathbf{s}}$ inside the AS will not affect[7,10] $\sigma_{\alpha\beta}$. N_e is the number of carriers in the conduction band inside $\Omega_{\mathbf{s}}$, and f is the Fermi distribution function. The velocity matrix elements in Eq.(1) are defined by

$$v^{\alpha}_{BA} = -\frac{i\hbar}{m} \int d^3x \chi^*_B(\mathbf{r}) \frac{\partial}{\partial x_\alpha} \phi_A(\mathbf{r} - \mathbf{R}_A), \quad (2)$$

and

$$w^{\alpha}_{AB} = -\frac{i\hbar}{m} \int d^3x \phi_A(\mathbf{r} - \mathbf{R}_A) \frac{\partial}{\partial x_\alpha} \chi^*_B(\mathbf{r}), \quad (3)$$

where E^0_A and ϕ_A are the eigenvalue and eigenfunction of localized state A. We will use letter A with or without a natural number subscript to denote a localized state,

similarly E_B^0 and χ_B are the eigenvalue and eigenfunction of extended state B. $I_{B_1A\pm}$ arise from integrating out the vibrational degrees of freedom, and are functions of external field frequency ω:

$$I_{B_1A\pm}(\omega) = \exp\{-\frac{1}{2}\sum_\alpha \coth\frac{\beta\hbar\omega_\alpha}{2}(\theta_\alpha^A)^2\}$$

$$\times \int_{-\infty}^{0} ds e^{is(\pm\omega+\omega_{AB_1})}$$

$$\exp\{\frac{1}{2}\sum_\alpha(\theta_\alpha^A)^2[\coth\frac{\beta\hbar\omega_\alpha}{2}\cos s\omega_\alpha - i\sin s\omega_\alpha]\}, \quad (4)$$

where $\omega_{AB} = (E_A^0 - E_B^0)/\hbar$, ω_α is the frequency of the α^{th} ($\alpha = 1, 2, \cdots 3\mathcal{N}$) normal mode, $\mathcal{N}$ is number of atoms inside $\Omega_{\mathbf{s}}$. Denote Θ_α^A as the shift in the origin of the α^{th} mode induced by the electron-phonon (e-ph) interaction in a localized state[6,7] A, $\theta_\alpha^A = \Theta_\alpha^A(M_\alpha\omega_\alpha/\hbar)^{1/2}$. To make the narration specific, we hereafter discuss conduction band transport only. For transport processes in the valence band, one may repeat the discussion *mutatis mutandis*.

To calculate conductivity strictly, one needs (i) the eigenvalues and eigenvectors of single-electron states and (ii) the eigenfrequencies and eigenvectors of the normal modes and the electron-phonon coupling. These can be approximately obtained by one step of *ab initio* molecular dynamics for an optimized configuration. Then one can compute (i) v_{BA}^α for all localized states and extended states; (ii) θ_α^A for all normal modes in each localized states; (iii) time integrals $I_{B_1A\pm}$ for a given ω; and (iv) sum over all localized states and extended states $\sum_{AB}$. Although the result obtained in this way should be accurate and predictive, it is useful to develop an approximate theory, which also provides functional dependence of transport on various material parameters.

In this paper, we will first present a tractable model for the conductivity and Hall mobility in AS. Then we will use this model to simplify the conductivity expressions obtained in the MRM for the three simplest transitions: LL, LE and EL transitions driven solely by external field, cf. Fig. 2a, 2b and 6a of [7]. The conductivity from EE transition caused by disorder has been solved in the coherent potential approximation[13,14], exhibits weak temperature dependence, and we will not consider it further.

The outline of the paper is as following. In Sec.II we describe our approximation for the lattice vibrations and e-ph in coupling. In Sec.III A, we first illustrate that the MRM conductivity can be put in the customary form of relaxation time approximation and of Greenwood formula. At moderately high temperature, we invoke an asymptotic expansion to simplify the time integrals $I_{B_1A\pm}$. Under the approximations introduced in Sec.II, one can (i) obtain the velocity matrix elements analytically; (ii) partially carry out the two-fold summations over the initial and final electronic states. The conductivity from EL transitions is obtained in Sec.III B. The conductivity from LL transitions is calculated in Sec.III C. The matrix elements of electronic velocity could be carried out in a spherical coordinate system analytically. The conductivity from the LE transitions is the same order of magnitude as those from the LL transitions. Below a crossover temperature T*, the later is larger; above T*, the former is larger. This phenomenon is the main reason for the kink in the experimental $\log_{10}\sigma$ vs. 1/T curve. As a demonstration, the numerical results for n-doped a-Si:H and a-Ge:H samples are given.

TABLE I: Parameters for vibrational spectrum

	B(GPa)	μ(GPa)	$\overline{c}(10^3\text{m/s})$	$k_D(\text{Å}^{-1})$	$\rho_m(\text{g/cm}^3)$
a-Si[12,16,17]	100	52	6.21	1.44	2.33
a-Ge[12,16,17]	75	41	3.08	1.38	5.33

II. APPROXIMATE IMPLEMENTATION OF MRM

A. Vibrations

To calculate the e-ph interaction for a localized state, we need the transformation matrix between the atomic displacements and normal modes[6]. Because most amorphous materials are isotropic[1,2] and only acoustic modes are important for the e-ph interaction in one component semiconductors[15], one can use the acoustic dispersion relation for the vibrational spectrum:

$$\omega_{\mathbf{k}} = \overline{c}k, \;\; k = |\mathbf{k}| \quad (5)$$

where $\omega_{\mathbf{k}}$ is the angular frequency for any mode characterized by wave vector $\mathbf{k}$. For every $\mathbf{k}$, there are one longitudinal and two transverse modes. We will use $\mathbf{k}\tau$ to label a normal mode, where $\tau = 1, 2, 3$ is the index of phonon branches[18]. Although translational invariance is destroyed in AS, standing wave modes are still well-defined. Here, $\overline{c}$ is the average speed of sound:

$$\frac{3}{\overline{c}^3} = \frac{2}{c_t^3} + \frac{1}{c_l^3}, \quad (6)$$

where c_t and c_l are the speeds of transverse and longitudinal waves which are determined by[18] the bulk modulus B and shear modulus μ. The cutoff wave vector $k_D = (6\pi^2 n_a)^{1/3}$ is determined by the number density $n_a = \mathcal{N}/V$ of atoms, where V is the volume of an AS, $\mathcal{N}$ is total number of atoms[19]. n_a can be inferred from the observed mass density ρ_m. For a-Si and a-Ge, ρ_m, B, μ[9,12], k_D and $\overline{c}$ are listed in Table I. For a-Si, the Debye frequency ω_D is 8.91×10^{13}Hz, not far from the observed cut-off frequency[20] 70meV$= 1.07 \times 10^{14}$Hz.

It is convenient to use $\{x_{3(j-1)+1}, x_{3(j-1)+2}, x_{3(j-1)+3}\}$ to represent the vibrational displacement vector $\mathbf{u}_j = \{u_{jx}, u_{jy}, u_{jz}\}$ for the j^{th} atom ($j = 1, 2, 3 \cdots \mathcal{N}$). Denote $\Theta_\alpha (\alpha = 1, 2, \cdots, 3\mathcal{N})$ as the normal coordinate of the α^{th} mode, so that the atomic displacements and the normal modes are related by

$$x_m = \sum_\alpha \Delta_{m\alpha}\Theta_\alpha,\ m = 1, 2, \cdots, 3\mathcal{N} \tag{7}$$

where Δ is the minor of the determinant $|\Lambda_{jl} - \omega^2 M_j \delta_{jl}|$ ($j, l = 1, 2, 3 \cdots 3\mathcal{N}$), Λ is the force constant matrix[21]. When we use $\mathbf{k}\tau$ to label modes, $\sum_\alpha \to \sum_{\mathbf{k}\tau}$.

For a localized state, the shifts in the origins of normal modes caused by the e-ph interaction are the key quantities to determine the reorganization energy for transitions involving the localized state[6]. The shift in origin is determined[6] by Λ^{-1}, Δ and the e-ph coupling constant. Λ^{-1} and Δ are complicated for a system with many atoms. To avoid using Λ^{-1} and find a more practical Δ, we use a continuum to model the discrete random network of AS. In a continuum one can classify the atomic vibrations according to possible standing wave modes. There is no reciprocal lattice for AS. Because a continuum is isotropic and has continuous translational symmetry, the wave vectors of the possible standing waves ($\mathbf{k}$ points) is uniformly distributed in the wave vector space (Debye sphere S_D). The $\mathcal{N}$ $\mathbf{k}$-points inside S_D correspond to $3\mathcal{N}$ vibrational modes.

The atomic displacement $\mathbf{u}$ at position $\mathbf{R}$ and time t satisfies the wave equation

$$\frac{1}{\overline{c}^2}\frac{\partial^2 \mathbf{u}(\mathbf{R}, t)}{\partial t^2} = \nabla^2 \mathbf{u}(\mathbf{R}, t). \tag{8}$$

The plane wave solution of Eq.(8) is[19]

$$\mathbf{u}(\mathbf{R}, t) = \frac{1}{\mathcal{N}^{1/2}} \sum_{\mathbf{k}\tau} e^{i\mathbf{k}\cdot\mathbf{R}} \mathbf{e}_{\mathbf{k}\tau} \Theta_{\mathbf{k}\tau} e^{-i(t\overline{c}k + \varphi_{\mathbf{k}\tau})}, \tag{9}$$

where $\mathbf{e}_{\mathbf{k}\tau}$ is the polarization vector of mode $\mathbf{k}\tau$. For a one-component system[19],

$$\mathbf{e}_{\mathbf{k}\tau} \cdot \mathbf{e}^*_{\mathbf{k}\tau'} = \delta_{\tau\tau'}. \tag{10}$$

$\Theta_{\mathbf{k}\tau}$ and $\varphi_{\mathbf{k}\tau}$ are the amplitude and phase of mode $\mathbf{k}\tau$, and are determined by the initial conditions. The inverse of Eq.(9) is

$$\Theta_{\mathbf{k}\tau} e^{-i(t\overline{c}k + \varphi_{\mathbf{k}\tau})} = \frac{1}{\mathcal{N}^{1/2}} \sum_{\mathbf{R}} \mathbf{u}(\mathbf{R}, t) \cdot \mathbf{e}^*_{\mathbf{k}\tau} e^{-i\mathbf{k}\cdot\mathbf{R}}. \tag{11}$$

The normal coordinate of mode $\mathbf{k}\tau$ is $\Theta_{\mathbf{k}\tau} e^{-i(t\overline{c}k + \varphi_{\mathbf{k}\tau})}$, so that

$$\Delta_{\mathbf{u}(\mathbf{R}), \mathbf{k}\tau} = \mathcal{N}^{-1/2} e^{i\mathbf{k}\cdot\mathbf{R}} \mathbf{e}_{\mathbf{k}\tau}, \tag{12}$$

and

$$(\Delta^{-1})_{\mathbf{k}\tau, \mathbf{u}(\mathbf{R})} = \mathcal{N}^{-1/2} e^{-i\mathbf{k}\cdot\mathbf{R}} \mathbf{e}^*_{\mathbf{k}\tau}. \tag{13}$$

TABLE II: Parameters for electronic state

	E_c(eV)	U(meV)	n_{loc}(Å^{-3})	Z	ε	q_{TF}(Å^{-1})	b
a-Si	0.5[30]	50[31]	5/10.86^3[32]	4	11.68	1.7	0.121
a-Ge	0.5	51	5/11.32^3	4	16	1.7	0.170

In other words, the $\mathbf{u}(\mathbf{R})^{\text{th}}$ column of matrix Δ^{-1} is the $(\mathbf{k}\tau)^{\text{th}}$ eigenvector belongs to the $(\mathbf{k}\tau)^{\text{th}}$ eigenvalue $(\omega_{\mathbf{k}\tau})^2 = (\overline{c}k)^2$ of the matrix of force constants. Eqs.(12,13) as consequences of Eq.(8) is contained in the Debye assumption (5).

B. Localized states

To obtain analytical expressions for the e-ph interaction in a localized state and the velocity matrix elements, we need reasonable and simple approximate wave functions for localized and extended states. We assume all localized states are spherically symmetric. The difference among localized states is expressed by the localization length[2]. For a localized state A, denote $\mathbf{R}_A$ as the position vector of the center, the normalized wave function is

$$\phi_A(\mathbf{r} - \mathbf{R}_A) = \pi^{-1/2} \xi_A^{-3/2} e^{-|\mathbf{r} - \mathbf{r}_A|/\xi_A}, \tag{14}$$

where $\mathbf{r}$ and ξ_A are the coordinate of electron and localization length[22]. Following Mott, ξ_A is determined by the eigenvalue E of localized state ϕ_A[22]:

$$\xi_E = \frac{bZe^2}{4\pi\epsilon_0\varepsilon}(E_c - E)^{-1}, \tag{15}$$

where Z is the effective nuclear charge of an atom core, ε is the static dielectric constant. E_c is the mobility edge, b is a dimensionless constant. b is determined by the shortest possible localization length $\xi_{\min}$ with $E = 0$. Realistic calculations of tail states are given in [23–27].

The parameters[1,12] for electron-core interaction and localized state are listed in Table II. In a-Si:H and a-Ge:H[1,12], the most localized states are associated with dangling bonds. The localization length is one half the average bond length: $\xi_{\min} = 2.35$Å$/2$ and 2.45Å$/2$. Using Eq.(15), one has $b = 0.121$ and 0.170. The measured value of mobility edge for a-Si is rather dispersed[28,29]: 0.2-2eV: we will take[30] $E_c = 0.5$eV. Fig.1 plots localization length vs. eigenenergy, we purposely left out a small neighborhood $[E_c - U, E_c)$ of E, where U is the Urbach energy for band tail. When ξ_E is larger than the linear size of a physical infinitesimal volume element[16] ($\sim$100Å), the corresponding localized state acts like an extended state for purpose of transport.

There is a distinction between a large polaron and a carrier in a weakly localized state with ξ several tens of Å. A large polaron can move freely before meeting a scatterer, while a localized carrier in AS is trapped in

the region where ϕ_A has support. To make a localized carrier move, thermal activation involving a reorganization of vibrational configuration is necessary[6].

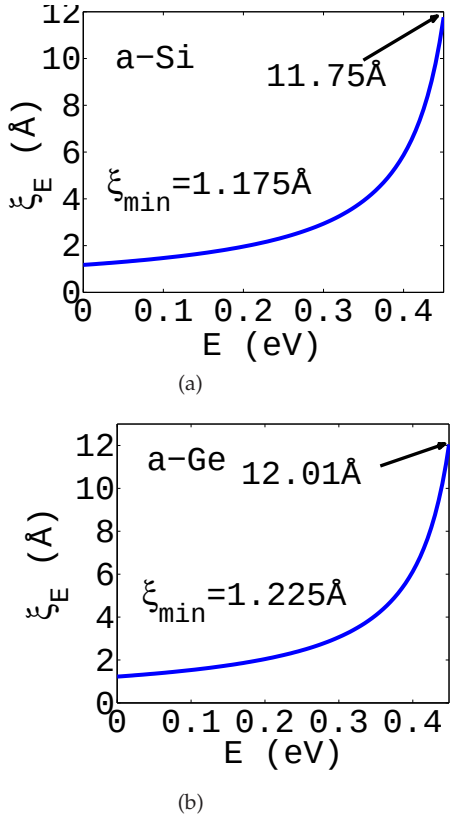

FIG. 1: Localization length as function of energy, 1(a): a-Si; 1(b): a-Ge.

Because (i) no translational invariance exists in an AS; and (ii) a localized electronic state is confined in some finite region, the spatial distribution of localized states needs special attention. For various macroscopic properties, an AS can be viewed as isotropic and uniform at a length scale larger than[16] 10nm (this effectively defines the physical infinitesimal volume element Ω). Therefore it is convenient to describe the spatial distribution of localized states in a spherical coordinate system. For a given origin and polar axis, the sum over localized states A_1 can be changed into an integral over a combined spatial and energetic distribution of localized states:

$$\sum_{A_1} \to \int_0^{R_c} R^2 dR \int_0^{\pi} \sin\theta d\theta \int_0^{2\pi} d\phi \int_{-\infty}^{E_c} dE f(R,\theta,\phi;E), \tag{16}$$

where R is the distance between the origin and the center $\mathbf{R}_{A_1}$ of a localized state ϕ_{A_1}, R_c is the radius of an AS sample, $f(R,\theta,\phi;E)$ is the number of localized states in a volume element defined by $(R, R+dR)$, $(\theta, \theta+d\theta)$ and $(\phi, \phi+d\phi)$ with energy $(E, E+dE)$, i.e. position dependent density of states. Since a volume element with a linear size of 10nm is representative for an AS, in the calculation of transport coefficients, one may replace the volume V of the entire AS sample with the volume Ω of a physical infinitesimal volume element. Then R_c is the radius of Ω.

In a physical infinitesimal volume Ω, various possible atomic configurations appear according to the proper statistical weights which would be found in a much larger sample. Therefore the coarse-grained average $\overline{f}$ of $f(R,\theta,\phi;E)$ over such a physical infinitesimal volume element is no longer position dependent: $\overline{f} = N(E)$, where $N(E)$ is the usual density of states. However the weight factors in Eq.(16) play an important role in determining transport properties. The reason is that although $\overline{f}$ is independent of (R,θ,ϕ), the transition amplitudes (velocity matrix elements) depend on the relative position of another localized state or on the wave vector direction of the involved extended state.

For many AS[33,34], in the range of band tail, the density of localized states satisfies

$$\overline{f}(R,\theta,\phi;E) = N(E) = \frac{n_{loc}}{U} e^{-(E_c-E)/U}, \tag{17}$$

where U is the Urbach energy, $n_{\rm loc}$ is the number of localized states per unit volume. The pre-exponential factor is determined from the requirement that the integral of $N(E)$ over all localized energy spectrum should be $n_{\rm loc}$. In general E_c and U take different values for the valence band and the conduction band[34]. Denote n as the carrier concentration, the Fermi energy E_F of a weakly doped AS is:

$$E_F = E_c + U \ln(n/2n_{loc}), \tag{18}$$

When $n \le 2n_{loc}$, all occupied states are localized at T= 0K. For a-Si, the conduction band energy spectrum (17) is illustrated in Fig.2. We can see from Fig.1(a) and

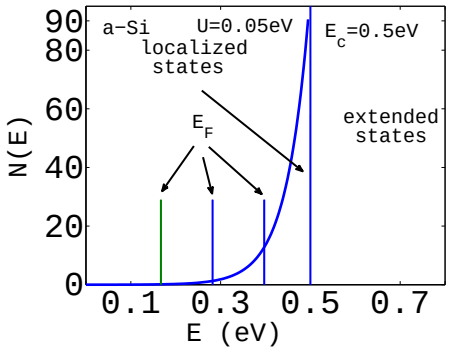

FIG. 2: Density of states of the conduction tail for n-doped a-Si samples: the first three vertical lines are the Fermi energy for $n = 10^{19}$, 10^{20} and 10^{21} cm^{-3}. The rightmost vertical line is the mobility edge.

Eq.(17) that most localized states in a-Si have a localization length in the range 6-12Å. In approximation (17), the density of states $N(E)$ of localized states reaches its

maximum at E_c. Therefore, the most probable localization length is $\overline{\xi} = cZe^2/(4\pi\epsilon_0\varepsilon U)$. For a-Si, $\overline{\xi} = 11.75$Å. This is consistent with various experiments[35–41].

Making use of relation (15), the integral over the energy eigenvalues of localized states is converted into an integral over localization lengths:

$$\int_{-\infty}^{E_c} dE_A N(E_A) \rightarrow \tag{19}$$

$$\frac{bZe^2 n_{loc}}{4\pi\epsilon_0\varepsilon U}\int_0^{\infty}\frac{d\xi}{\xi^2}\exp(-\frac{bZe^2}{4\pi\epsilon_0\varepsilon U\xi}).$$

Comparing Eq.(16) with the sum over states $\sum_{\mathbf{k}} \rightarrow \int_{BZ}\frac{Vd^3k}{(2\pi)^3}$ in a crystal is helpful, where $\mathbf{k}$ is the wave vector of a Bloch state in Brillouin zone, V is volume of the crystal. The matrix elements behind $\sum_{\mathbf{k}}$ may depend on the direction of $\mathbf{k}$, $d^3k = k^2dk\sin\theta_{\mathbf{k}}d\theta_{\mathbf{k}}d\phi_{\mathbf{k}}$ takes into account the dependence on the two wave vectors of two Bloch states.

C. Extended states

If one imagines that an AS is obtained from deforming its reference crystal, an extended state in the AS can be viewed as a superposition of a principal Bloch wave with a given wave vector and its scattered secondary waves[42,43]. The scattered waves are produced by scattering the principal Bloch wave with the disorder potential (the difference between the potential energy in the AS and that in its reference crystal)[42,43]. Excepting the EE transitions driven by external field, we may approximate an extended state $\chi_{B_1}(\mathbf{r})$ by a plane wave with certain momentum $\mathbf{p}$, and its eigenenergy is that of the plane wave:

$$\chi_{B_1} = V^{-1/2}e^{i\mathbf{p}\cdot\mathbf{r}/\hbar}, \quad E_{B_1} = p^2/2m, \tag{20}$$

where V is the volume of AS sample, the energy zero-point of extended states is at the mobility edge E_c. An extended state in an AS is labeled by the wave vector of its principal Bloch wave. The sum over extended states becomes an integral over momentum: $\sum_{B_1} \rightarrow \int\frac{Vd^3p}{(2\pi\hbar)^3}$.

D. Interaction between a carrier and an atomic core

In a solid, the attraction to an electron from an atomic core may be crudely approximated by a screened Coulomb potential[19]

$$V(\mathbf{r}) = \frac{Ze^2}{4\pi\epsilon_0\varepsilon}\frac{e^{-q_{TF}r}}{r}, \tag{21}$$

where $\mathbf{r}$ is the position of electron relative to an atomic core. $q_{TF} = 2.95(r_s/a_0)^{-1/2}$Å^{-1} is the Thomas-Fermi wave vector, is determined by the carrier density. r_s/a_0 is a number about 2 to 6. For a-Si:H[1] and a-Ge[12], we take the value for c-Si and c-Ge: $q_{TF} = 1.7$Å^{-1}.

E. Electron-phonon coupling in a localized state

We consider the mean e-ph interaction in a localized state ϕ_A. The e-ph interaction Hamiltonian is

$$H_{\text{e-ph}} = \sum_{n\sigma} u_{n\sigma}\frac{\partial V(\mathbf{r}-\mathbf{R}_n)}{\partial X_{n\sigma}},\ \sigma = x,y,z, \tag{22}$$

where $\mathbf{R}_n$ (X_{nx}, X_{ny}, X_{nz}) is the position vector of the n^{th} atom, $u_{n\sigma}$ is the σ^{th} Cartesian component of vibrational amplitude of the n^{th} atom. Usually the average e-ph interaction in state ϕ_A is written in a linear coupling form[44]

$$\int d^3x\phi_A^*(\mathbf{r}-\mathbf{R}_A)H_{\text{e-ph}}\phi_A(\mathbf{r}-\mathbf{R}_A) = -\sum_{n\sigma}u_{n\sigma}g_{n\sigma}^A, \tag{23}$$

where $g_{n\sigma}^A$ is the e-ph coupling constant in state ϕ_A. Because we consider only localized state ϕ_A, it is convenient to shift the origin of coordinate to the center $\mathbf{R}_A$ of ϕ_A. In Eq.(22), we sum over all the atoms in V of an AS sample. In addition, the factors $V(\mathbf{r}-\mathbf{R}_n)$ and $\phi_A(\mathbf{r}-\mathbf{R}_A)$ in the integrand of Eq.(23) involve two atoms, directly integrating over coordinate is difficult (requiring ellipsoidal coordinate system). To obtain the coupling constant $g_{n\sigma}^A$, we Fourier transform $\partial V(\mathbf{r}-\mathbf{R}_n)/\partial X_{n\sigma}$ in the LHS of Eq.(23), first carry out the integral in coordinate $\mathbf{r}$, then execute the integral over wave vector $\mathbf{q}$. The final result is:

$$g_{n\sigma}^A = \frac{16(Ze^2/4\pi\epsilon_0\varepsilon)}{\xi^4}\frac{X_{n\sigma}}{R_n^2}\{\frac{R_n}{2}\frac{e^{-2R_n/\xi}}{q_{TF}^2-(2/\xi)^2}$$

$$+[\frac{q_{TF}e^{-q_{TF}R_n}-(2/\xi)e^{-2R_n/\xi}}{[(2/\xi)^2-q_{TF}^2]^2}-\frac{\xi}{8}\frac{e^{-2R_n/\xi}}{q_{TF}^2-(2/\xi)^2}]$$

$$+\frac{1}{R_n}[\frac{e^{-q_{TF}R_n}-e^{-2R_n/\xi}}{[(2/\xi)^2-q_{TF}^2]^2}-\frac{\xi^2}{16}\frac{e^{-2R_n/\xi}}{q_{TF}^2-(2/\xi)^2}]\}, \tag{24}$$

where $R_n = |\mathbf{R}_n - \mathbf{R}_A|$ is the distance between the n^{th} atom to the center $\mathbf{R}_A$ of localized state ϕ_A. The first term decays exponentially, the second and the third term contain additional decay factors R_n^{-1} and R_n^{-2} respectively. Since we are concerned only with localized state ϕ_A, hereafter we drop the subscript A on ξ and g.

F. Polaron formation

The static displacements of atoms induced by the e-ph interaction measure the strength of e-ph interaction and

determine whether the e-ph coupling should be treated as a perturbation or be included in the zeroth order Hamiltonian[6]. The static displacement of the m^{th} atomic degree of freedom caused by the e-ph interaction in localized state ϕ_A is[6]

$$x_m^{A0} = \sum_p (\Lambda^{-1})_{mp} g_p^A,\ m,p = 1,2,\cdots 3\mathcal{N}, \tag{25}$$

where Λ^{-1} is the inverse of force constant matrix. The shift Θ_α^A in origin of the α^{th} ($\alpha = 1,2,\cdots 3\mathcal{N}$) mode by the carrier localized in state ϕ_A is[6]

$$\Theta_\alpha^A = \sum_m (\Delta^{-1})_{\alpha m} x_m^{A0}. \tag{26}$$

This has the physical interpretation of the polaronic relaxation due to the e-ph coupling.

If Λ^{-1} and Δ^{-1} were known analytically, we could use Eq.(25) to find $\{x_m^{A0}\}$, and then use Eq.(26) to find $\{\Theta_\alpha^A\}$. The continuum model in Sec.II A allows us to first find the shifts in origins $\{\Theta_\alpha^A\}$ of normal modes in a localized state. Then static displacements $\{x_m^{A0}\}$ can be obtained from Eq.(7). In the continuum model, the normal modes are labeled by wave vectors $\mathbf{k}$. Substitute Eq.(25) into Eq.(26), notice $\Delta^{-1}\Lambda^{-1} = W^{-1}\Delta^T$, where $(W^{-1})_{\alpha\beta} = \delta_{\alpha\beta} M_\alpha^{-1}\omega_\alpha^{-2}$, one concludes that

$$\Theta_{\mathbf{k}\tau}^A = M_{\mathbf{k}}^{-1}\omega_{\mathbf{k}}^{-2} \sum_{n\sigma} g_{n\sigma}^A \Delta_{n\sigma,\mathbf{k}\tau}, \tag{27}$$

where $n = 1,2,3\cdots\mathcal{N}$ and $\sigma = x,y,z$. Substituting Eq.(12) into Eq.(27) and replacing the sum by an integral over all space, Eq.(27) becomes

$$\Theta_{\mathbf{k}\tau}^A = \frac{\mathrm{Re}\sum_\sigma \int_V d^3X g_{\mathbf{R}\sigma}^A e_{\mathbf{k}\tau}^\sigma e^{i\mathbf{k}\cdot\mathbf{R}}}{\mathcal{N}^{1/2} M_{\mathbf{k}} \omega_{\mathbf{k}}^2 \Omega_a}, \tag{28}$$

where $\Omega_a = V/\mathcal{N}$ is the average volume occupied by one atom. For a-Si and a-Ge[12,19], $\Omega_a \approx (5.43\text{Å})^3/4$ and $(5.66\text{Å})^3/4$. Eq.(28) expresses the shift $\Theta_{\mathbf{k}}^A$ in the origin of normal mode $\mathbf{k}$ with the e-ph coupling constant $g_{n\sigma}^A$. We take $\mathbf{k}$ as the polar axis (z axis) and transform to a spherical coordinate system, because the integrand of Eq.(28) does not contain azimuthal angle ϕ, $\{g_{nx}^A\}$ and $\{g_{ny}^A\}$ do not contribute to $\Theta_{\mathbf{k}\tau}^A$. Only when $\mathbf{g}_n^A$ has a component along $\mathbf{k}$, does it contribute to $\Theta_{\mathbf{k}\tau}^A$. The integrations over the R^{-2} and R^{-3} terms in Eq.(24) are purely imaginary, and do not contribute to $\Theta_{\mathbf{k}}^A$. The origin shift of mode $\mathbf{k}\tau$ induced by the e-ph interaction in localized state ϕ_A is:

$$\Theta_{\mathbf{k}\tau}^A = \frac{1}{\mathcal{N}^{1/2} M k^2 \overline{c}^2} \frac{2^7 \pi Z e^2/(4\pi\epsilon_0\varepsilon\Omega_a\xi^5)}{[q_{TF}^2 - (2/\xi)^2][(2/\xi)^2 + k^2]^2}. \tag{29}$$

Because we take AS to be an isotropic continuous medium, $\Theta_{\mathbf{k}\tau}^A$ depends only on the magnitude k. The k^{-2} divergence in Eq.(29) when $k \to 0$ is caused by the Debye spectrum ($\omega_{\mathbf{k}} = \overline{c}k$). In a Debye model, the number of modes per unit volume per unit angular frequency interval is[19] $(2\pi^2\overline{c})^{-1}3k^2$ when $k < k_D$. The shift is smaller for higher wave number, decays with wave vector $\mathbf{k}$ as $[(2/\xi)^2 + k^2]^{-2}$. Because for all materials[19] $q_{TF} \sim 1.2 - 2.1\text{Å}^{-1}$, while $\xi > 2$Å for localized states caused by topological disorder[22], the factor $[q_{TF}^2 - (2/\xi)^2]$ in the denominator of Eqs.(24,29,31,34,37) will not lead to a divergent result.

Eq.(29) exhibits two obvious features: (i) $\Theta_{\mathbf{k}}^A > 0$ for every mode $\mathbf{k}$; (ii) if $\xi_{A_1} < \xi_{A_2}$, then $\Theta_{\mathbf{k}}^{A_1} > \Theta_{\mathbf{k}}^{A_2}$ for every mode $\mathbf{k}$. We have shown that three-state conduction processes which are first order in residual interactions, are the same order of magnitude as the two-states processes discussed here[7]. Also, in the lowest order self-consistent approximation, three- and four-state processes must be included in the Hall mobility calculation[7]. Some of the aforementioned transport processes involve at least two localized states. To carry out asymptotic expansion at high temperature for such processes, the features (i) and (ii) are essential.

The static atomic displacements in localized state A can be found from Eqs.(26,29):

$$x_\sigma^{0A}(\mathbf{R}) = \frac{\mathcal{N}^{1/2}\Omega_a}{(2\pi)^3} \sum_{\tau=1}^{3} \int d^3k e^{i\mathbf{k}\cdot\mathbf{R}} \Theta_{\mathbf{k}\tau}^A e_{\mathbf{k}\tau}^\sigma. \tag{30}$$

Next, substitute Eq.(29) into Eq.(30) and carry out the integral. One finds the displacement x^{0A} along the radial direction for an atom at $\mathbf{R}$ caused by e-ph interaction in a localized state:

$$x^{0A}(\mathbf{R}) = \frac{4}{M\overline{c}^2} \frac{Z^* e^2/4\pi\epsilon_0\varepsilon}{\xi[q_{TF}^2 - (2/\xi)^2]} \frac{1 - \frac{1}{2}e^{-2R/\xi}}{R}, \tag{31}$$

where we have let $k_D \to \infty$ to obtain an analytic result. It is interesting to notice that Eq.(31) is similar to the wave function of large polaron in strong coupling limit, cf. pp513-523 of [15].

Fig.3(a) is an illustration of Eq.(31) for a-Si at $\xi = 11.75$Å and 23.50Å (5 and 10 times bond length). We observe that the more localized (smaller ξ) the state, the larger the atomic displacements, i.e. the stronger e-ph interaction (larger atomic displacements). This agrees with previous experiments and simulations[45,46]. For the hardest mode[20] $\omega = 70$meV of a-Si, the amplitude $A_0 = (\hbar/M\omega)^{1/2}$ of zero-point vibration is 0.046Å, the amplitude $A_{th} = (k_B T/M\omega^2)^{1/2}$of thermal vibration at 300K is 0.028Å. Considering these two peaks of the a-Si phonon spectrum are at[20] 20 meV ($A_0 = 0.086$Å, $A_{th} = 0.098$Å) and 60 meV ($A_0 = 0.050$Å, $A_{th} = 0.033$Å), the static displacements of atoms estimated in Eq.(31) are twice the amplitude of vibrations. Comparing the root mean square of bond length fluctuation 0.2Å (geometric disorder) from *ab initio* molecular dynamics

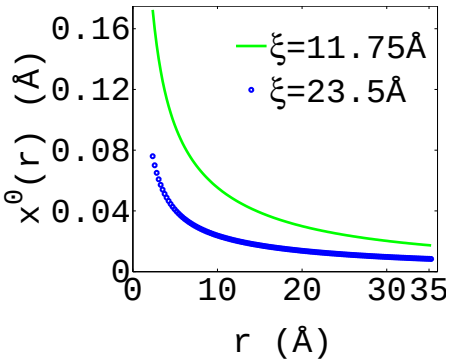

(a)

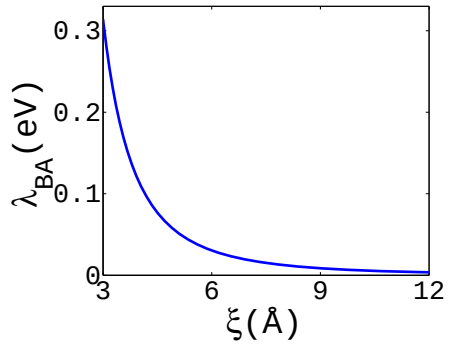

(b)

FIG. 3: 3(a): Static displacements $x^0(\mathbf{r})$ of atoms in a localized state ϕ_A as function of the distance r to the center of ϕ_A in a-Si: solid line is for $\xi = 11.75$Å, circle line is for $\xi = 23.5$Å. The displacements are larger in a more localized state. 3(b): The binding energy caused by e-ph interaction as function of localization length. The binding energy is larger for a more localized state.

simulation[23], the approximate acoustic dispersion relation Eq.(5) somewhat overestimates the long wave contribution in Eqs.(28,29,30,31).

G. Reorganization energy

Unlike a carrier in an extended state, a carrier in a localized state is confined by the disorder potential. Beyond that, the e-ph interaction produces[6] an additional binding energy E_b^A to a localized carrier in ϕ_A:

$$E_b^A = \frac{1}{2}\sum_\alpha M_\alpha \omega_\alpha^2 (\Theta_\alpha^A)^2. \tag{32}$$

Because the reorganization energy measures the energy shift from initial vibrational configuration to the final vibrational configuration, E_b^A is the same as[6] the reorganization energy λ_{BA} of LE transition $\phi_A \to \chi_B$ and the reorganization energy λ_{AB} of EL transition $\chi_B \to \phi_A$: $\lambda_{AB} = \lambda_{BA} = E_b^A$. For the continuous medium model, the sum over modes in Eq.(32) may be converted to an integral over the Debye sphere in spherical coordinate system (k, θ', ϕ'):

$$\lambda_{AB} = \frac{\mathcal{N}\Omega_a}{2(2\pi)^3}\sum_{\tau=1}^{3}\int_0^{k_D} dk k^2 \times \tag{33}$$

$$\int_0^\pi d\theta' \sin\theta' \int_0^{2\pi} d\phi' M k^2 \overline{c}^2 (\Theta_{\mathbf{k}\tau}^A)^2.$$

Owing to spherical symmetry in Eq.(33), the direction of polar axis is arbitrary. Substituting Eq.(29) into Eq.(33) and carrying out the integral, one finds:

$$\lambda_{AB} = 2\pi \frac{(2^7\pi Z^* e^2/4\pi\epsilon_0\varepsilon)^2\xi}{2^7 M\overline{c}^2\Omega_a[(\xi q_{TF})^2 - 4]^2} \tag{34}$$

$$\times\{\frac{15}{48}\tan^{-1}\frac{k_D\xi}{2} + \frac{k_D\xi[1+(\frac{k_D\xi}{2})^2]^{-1}}{12}\times$$

$$([1+(\frac{k_D\xi}{2})^2]^{-2} + \frac{5}{4}[1+(\frac{k_D\xi}{2})^2]^{-1} + \frac{15}{8})\}.$$

Fig.3(b) displays the change in binding energy with localization length. We can see that more localized states have larger binding energy. In other words, when a carrier leaves or enters a more localized state, the required reorganization energy is larger, the corresponding LE and EL transitions are more hindered.

The reorganization energy $\lambda_{A_2A_1}$ for LL transition $\phi_{A_1} \to \phi_{A_2}$ satisfies a reciprocity condition[6] $\lambda_{A_1A_2} = \lambda_{A_2A_1}$, where

$$\lambda_{A_2A_1} = \frac{1}{2}\sum_\alpha M_\alpha\omega_\alpha^2(\Theta_\alpha^{A_2} - \Theta_\alpha^{A_1})^2. \tag{35}$$

Eq.(35) can be expressed as

$$\lambda_{A_2A_1} = |E_b^{A_1}| + |E_b^{A_2}| - B_{A_2A_1}, \tag{36}$$

where $E_b^{A_1}$ is obtained from Eq.(34) by replacing ξ with ξ_1, ξ_1 is the localization length of ϕ_{A_1}. $B_{A_2A_1} = \sum_\alpha \hbar\omega_\alpha\theta_\alpha^{A_2}\theta_\alpha^{A_1}$ is the interference term:

$$B_{A_2A_1} = \frac{2^7\pi Z^* e^2/4\pi\epsilon_0\varepsilon}{\Omega_a\xi_1^5[q_{TF}^2 - (2/\xi_1)^2]}\frac{2^7\pi Z^* e^2/4\pi\epsilon_0\varepsilon}{\xi_2^5[q_{TF}^2 - (2/\xi_2)^2]} \tag{37}$$

$$\times\frac{4\pi}{M\overline{c}^2}\{[(2/\xi_2)^2 - (2/\xi_1)^2]^{-2}[\frac{\xi_1^3}{16}\tan^{-1}\frac{k_D\xi_1}{2}$$

$$+\frac{k_D\xi_1^4}{8(k_D^2\xi_1^2+4)} + \frac{\xi_2^3}{16}\tan^{-1}\frac{k_D\xi_2}{2} + \frac{k_D\xi_2^4}{8(k_D^2\xi_2^2+4)}]$$

$$-2[(2/\xi_2)^2 - (2/\xi_1)^2]^{-3}[\frac{\xi_1}{2}\tan^{-1}\frac{k_D\xi_1}{2} - \frac{\xi_2}{2}\tan^{-1}\frac{k_D\xi_2}{2}]\}.$$

Eqs.(34,36,37) determined the reorganization energy $\lambda_{A_2A_1}$ for LL transition $\phi_{A_1} \to \phi_{A_2}$.

III. CONDUCTIVITY FROM LE AND EL TRANSITIONS DRIVEN SOLELY BY FIELD

In this section we assemble the approximations of the proceeding section to estimate the various contributions to the conductivity.

A. LE transitions driven by field

1. *Connection to relaxation time approximation and Kubo-Greenwood formula*

Inside the summation of Eq.(1), only electronic degrees of freedom appear. Each term can be written as:

$$\begin{cases} \text{Re} \\ \text{Im} \end{cases} \sigma^{BA}_{\alpha\beta}(\omega) = (m^{BA}_{eff})^{-1}_{\alpha\beta} n e^2 \tau^{BA}_{\pm}(\omega), \tag{38}$$

where $n = N_e/\Omega_s$ is the carrier density,

$$\tau^{BA}_{\pm}(\omega) = \text{Im}\, i[I_{BA+} \pm I_{BA-}]$$

may be viewed as a relaxation time, the real part of conductivity takes plus sign, the imaginary part takes the minus sign. Here

$$(m^{BA}_{eff})^{-1}_{\alpha\beta} = -\frac{(w^{\alpha}_{AB} - v^{\alpha}_{BA})(v^{\beta}_{BA})^*}{2(E^0_A - E^0_B)}, \tag{39}$$

may be interpreted as the inverse of the effective mass matrix tensor for transition $\phi_A \rightarrow \chi_B$. In this sense, $\sigma^{B_1A}_{\alpha\beta}(\omega)$ is a generalization of the energy dependent conductivity[2] $\sigma^{E}_{\alpha\beta}(\omega)$. With this notation, Eq.(1) becomes

$$\sigma_{\alpha\beta}(\omega) = \sum_{AB_1} \sigma^{B_1A}_{\alpha\beta}(\omega)[1 - f(E_{B_1})]f(E_A), \tag{40}$$

a generalization of Kubo-Greenwood formula, Eq.(2.11) of [2,49]. This shows how a kinetic approach may be properly generalized to AS.

2. *High temperature approximation of the time integral $I_{BA\pm}$*

To calculate $I_{BA\pm}(\omega)$ defined by Eq.(4), we change the integration variable from s to t: $s = t - i\beta\hbar/2$. Eq.(4) becomes

$$I_{BA\pm}(\omega) = \exp\{-\frac{1}{2}\sum_{\alpha} \coth\frac{\beta\hbar\omega_\alpha}{2}(\theta^A_\alpha)^2\} e^{\beta\hbar(\pm\omega+\omega_{AB})/2}$$

$$\int_{-\infty+i\beta\hbar/2}^{i\beta\hbar/2} dt e^{it(\pm\omega+\omega_{AB})}$$

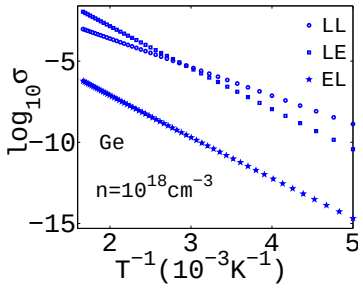

(a)

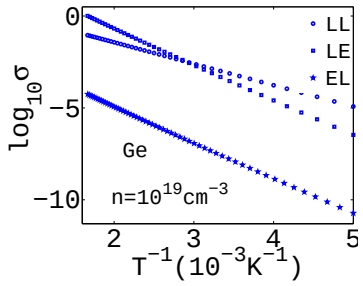

(b)

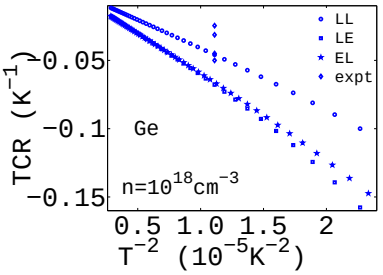

(c)

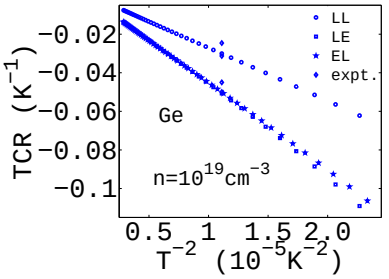

(d)

FIG. 4: Conductivity and TCR as functions of temperature in two n-doped a-Ge:H samples at $\omega = 0$. The experimental values are taken from [47,48].

$$\exp\{\frac{1}{2}\sum_{\alpha}(\theta^A_\alpha)^2 \operatorname{csc} h\frac{\beta\hbar\omega_\alpha}{2}\cos t\omega_\alpha\}. \tag{41}$$

If we view t as a complex variable, the saddle point of $\frac{1}{2}\sum_\alpha(\theta^A_\alpha)^2 \operatorname{csc} h\frac{\beta\hbar\omega_\alpha}{2}\cos t\omega_\alpha$ is at $(0,0)$. Because the integrand in Eq.(41) is analytic in the whole complex-t plane, we can deform the integral path from $(-\infty + i\beta\hbar/2, 0 + i\beta\hbar/2]$ to a new path C_1+C_2+C_3 crossing the

saddle point $(0,0)$, where C_1: $(-\infty + i\beta\hbar/2, -\infty + i0]$, C_2: $(-\infty, 0]$, C_3: $(0 + i0, 0 + i\beta\hbar/2]$. Because of the external field and residual interactions being adiabatically introduced[7], the integration along C_1 is zero. When $k_BT \geq \hbar\overline{\omega}$ ($\overline{\omega}$ is the frequency of the first peak in phonon spectrum), $\sum_\alpha(\theta_\alpha^A)^2 k_BT/\hbar\overline{\omega}$ is large. The integrals along C_2 and C_3 can be asymptotically calculated by the Laplace method[50]. The final result for $I_{BA\pm}$ is

$$I_{BA\pm}(\omega) = i\hbar/\lambda_{BA} \tag{42a}$$

$$+\frac{\hbar e^{\beta\hbar(\pm\omega+\omega_{AB})/2 - y_\pm^{BA} - \lambda_{BA}/4k_BT}}{(k_BT\lambda_{BA})^{1/2}}[\frac{\sqrt{\pi}}{2} - iA(y_\pm^{BA})],$$

where

$$y_\pm^{BA} = \frac{[\hbar(\pm\omega + \omega_{AB})]^2}{4\lambda_{BA}k_BT}, \quad \lambda_{BA} = \frac{1}{2}\sum_\alpha \hbar\omega_\alpha(\theta_\alpha^A)^2, \tag{43}$$

and

$$A(y_\pm) = \begin{cases} \sum_{n=0}^{\infty} \frac{y_\pm^{n+1/2}}{n!(2n+1)}, \text{ if } y_\pm \leq 1 \\ \frac{e^{y_\pm}}{2\sqrt{y_\pm}}[1 + \sum_{n=1}^{\infty} \frac{(2n-1)!!}{2^n y_\pm^n}], \text{ if } y_\pm > 1 \end{cases}. \tag{44}$$

The applicable condition for a-Si is T$>$ 232K[20,51,52]; for a-Ge is T$>$ 115K[51–53].

3. Velocity matrix elements

Under the approximations in Sec.II B and II C, the velocity matrix elements in Eq.(2) can be obtained by changing the integration variable from $\mathbf{r}$ to $\mathbf{r}' = \mathbf{r} - \mathbf{R}_A$, and introducing a spherical coordinate system with $\mathbf{R}_A$ as the origin and $\mathbf{p}$ as polar axis. One can show that $v_{B_1A}^x = v_{B_1A}^y = 0$, i.e. for the velocity components perpendicular to $\mathbf{p}$, the matrix elements are zero:

$$v_\perp^{B_1A} = 0. \tag{45}$$

The matrix element of v^z (the velocity component parallel to $\mathbf{p}$) is

$$v_\parallel^{B_1A} = v_{B_1A}^z = \frac{p}{m}8\pi^{1/2}\frac{e^{-i\mathbf{p}\cdot\mathbf{R}_A/\hbar}V^{-1/2}\xi^{3/2}}{(1 + p^2\xi^2/\hbar^2)^2}. \tag{46}$$

Similarly,

$$w_\parallel^{AB_1} = w_{AB_1}^z = -\frac{p}{m}8\pi^{1/2}\frac{e^{-i\mathbf{p}\cdot\mathbf{R}_A/\hbar}V^{-1/2}\xi^{3/2}}{(1 + p^2\xi^2/\hbar^2)^2}. \tag{47}$$

Substitute Eqs.(46,47) into Eq.(39), and the inverse of the effective mass tensor becomes

$$(m_{eff}^{B_1A-1})_{\alpha\beta} = \frac{m^{-1}p_\alpha p_\beta}{m(E_{B_1}^0 - E_A^0)}\frac{32\pi\xi^3V^{-1}}{(1 + p^2\xi^2/\hbar^2)^4}. \tag{48}$$

Since for each Cartesian component[2],

$$\langle\chi_B|x_\alpha|\phi_A\rangle = \frac{i\hbar\langle\chi_B|v_\alpha|\phi_A\rangle}{(E_A - E_B)}, \ \alpha = x, y, z, \tag{49}$$

from (45) and (46), one has

$$\langle\chi_B|r_\perp|\phi_A\rangle = 0 \text{ and } \langle\chi_B|r_\parallel|\phi_A\rangle = \frac{i\hbar v_\parallel^{BA}}{(E_A - E_B)}. \tag{50}$$

4. Relation to kinetic method

Because ϕ_A vanishes at $x_\alpha = \pm\infty$ ($\alpha = x, y, z$), by means of partial integration, one can show that $w_{AB}^\alpha = -v_{BA}^\alpha$. Then

$$(w_{AB}^\alpha - v_{BA}^\alpha)(v_{BA}^\beta)^* = -2v_{BA}^\alpha(v_{BA}^\beta)^* = -\frac{2}{3}v_{BA}^\alpha(v_{BA}^\alpha)^*\delta_{\alpha\beta}, \tag{51}$$

the last step is correct only for a cubic or isotropic body. For such a body, the product of two matrix elements is a real number. From the requirement that $\mathrm{Re}\,\sigma_{\alpha\beta}$ and $\mathrm{Im}\,\sigma_{\alpha\beta}$ are real numbers, we only require

$$\mathrm{Re}[I_{BA+} \pm I_{BA-}] = \frac{\sqrt{\pi}\hbar}{2(k_BT\lambda_{BA})^{1/2}} \tag{52}$$

$$\times[e^{-\frac{\lambda_{BA}}{4k_BT}[1+\frac{(\hbar\omega_{BA}-\hbar\omega)}{\lambda_{BA}}]^2} \pm e^{-\frac{\lambda_{BA}}{4k_BT}[1+\frac{(\hbar\omega_{BA}+\hbar\omega)}{\lambda_{BA}}]^2}]$$

in expression (1). The temperature dependence (52) is the same as that obtained from the kinetic method[6], although the Landau-Peierls condition is *not* satisfied. This is a coincidence caused by two factors. First, for LE, EL, LL and EE transitions driven by external field, the contribution to conductivity has the form of Eq.(1). Thus only the real part of the one dimensional time integral plays a role. In contrast to Eq.(4), in the corresponding kinetic expression[6], the upper limit of time integral is ∞ (long time limit) rather than 0. Second, because in both cases we apply an asymptotic expansion to calculate the time integral at high temperature, at leading order, the real part of (4) is half the corresponding time integral in kinetic theory. The difference in temperature dependence only appears in subdominant terms.

When transfer integrals or e-ph interaction are involved at first order, various transport processes are the same order of magnitude as the processes discussed here (zero-order in residual interaction). In these first-order processes, it is the imaginary part of a two-fold time integral that contribute to conductivity cf. [7]. Some of these first order processes do not appear in kinetic models. Even for the processes expected from kinetic theory, the temperature dependence derived in the MRM is different from that derived from kinetic theory.

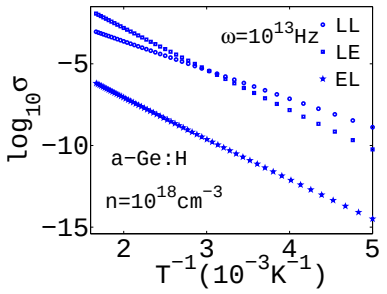

(a)

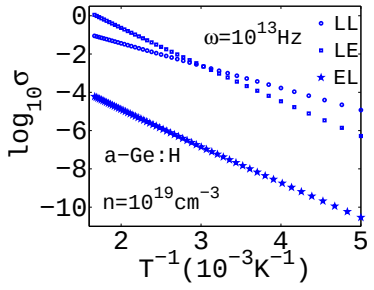

(b)

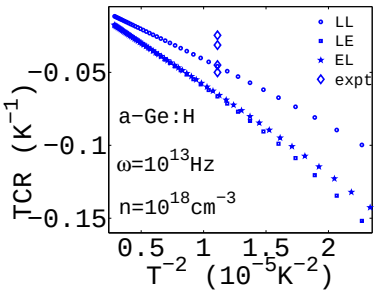

(c)

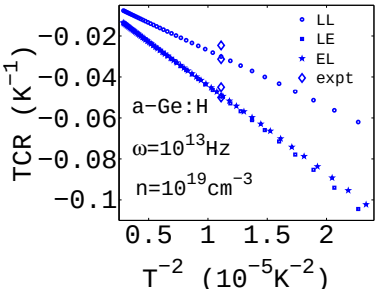

(d)

FIG. 5: Conductivity and TCR as functions of temperature in two n-doped a-Ge:H samples at $\omega = 10^{13}$ Hz. The experimental values are taken from [47,48].

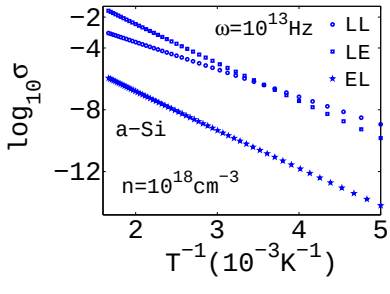

(a)

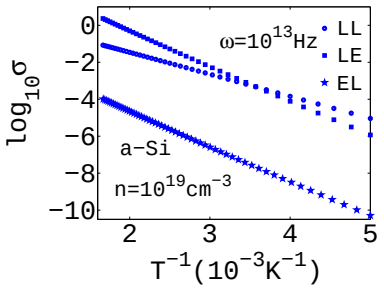

(b)

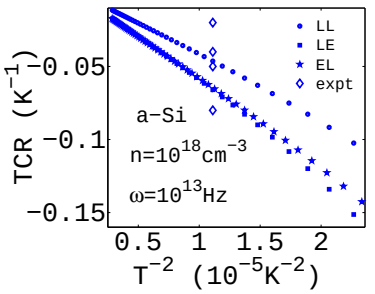

(c)

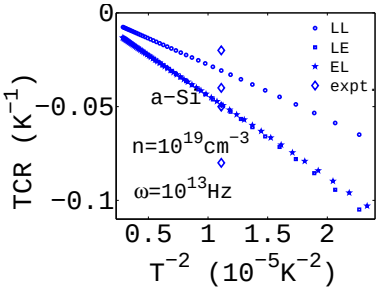

(d)

FIG. 6: Conductivity and TCR as functions of temperature in two n-doped a-Si:H samples at $\omega = 10^{13}$ Hz. The experimental values are taken from [55]

5. *Summation over electronic states*

To carry out the sum over the final extended states and average over initial localized states, we first carry out $\sum_B$ for a fixed localized state A. We take the center $\mathbf{R}_A$ of $\phi_A(\mathbf{r}-\mathbf{R}_A)$ as the origin of coordinates, the incident direction $\mathbf{k}/|\mathbf{k}|$ of electromagnetic wave as polar axis (z axis), the directions $(\boldsymbol{\epsilon}_1, \boldsymbol{\epsilon}_2)$ of two linear polarization vectors as x and y axis respectively. The incident field is expressed as

$$\mathbf{F} = F_1\boldsymbol{\epsilon}_1 + F_2\boldsymbol{\epsilon}_2 + 0\mathbf{k}/|\mathbf{k}|. \tag{53}$$

Consider an extended state (a wave packet propagating along $\mathbf{p}$) $V^{-1/2}e^{i\mathbf{p}\cdot\mathbf{r}/\hbar}$, here for simplicity we neglected

other waves with wave vectors close to $\mathbf{p}$. We can select an orthogonal frame ($\mathbf{l}$, $\mathbf{m}$, $\mathbf{n}$), where $\mathbf{n} = \mathbf{p}/|\mathbf{p}|$, $\mathbf{l}$ and $\mathbf{m}$ are two unit vectors perpendicular to each other and perpendicular to $\mathbf{n}$. The position vector $\mathbf{r}$ of electron can be resolved as

$$\mathbf{r} = r_{\perp 1}\mathbf{l} + r_{\perp 2}\mathbf{m} + r_{\parallel}\mathbf{n}. \quad (54)$$

According to Eq.(50), one has

$$\langle \chi_B|\mathbf{r}|\phi_A\rangle = \mathbf{n}\langle \chi_B|r_{\parallel}|\phi_A\rangle. \quad (55)$$

The matrix elements of the perturbation of external field is simplified to

$$\langle \chi_B|\mathbf{F}\cdot\mathbf{r}|\phi_A\rangle = \mathbf{F}\cdot\mathbf{n}\langle \chi_B|r_{\parallel}|\phi_A\rangle. \quad (56)$$

$$= \sin\theta(F_1\cos\phi + F_2\sin\phi)\frac{i\hbar v_{\parallel}^{BA}}{(E_A - E_B)},$$

where θ is the inclination angle of $\mathbf{p}$ relative to $\mathbf{k}$, ϕ is the azimuth angle of the orthogonal projection of $\mathbf{p}$ on plane $(\boldsymbol{\epsilon}_1, \boldsymbol{\epsilon}_2)$ relative to $\boldsymbol{\epsilon}_1$. In this coordinate system,

$$\sum_{B_1} \to \frac{V}{(2\pi\hbar)^3}\int_0^{\infty} dp p^2 \int_0^{\pi} d\theta \sin\theta \int_0^{2\pi} d\phi. \quad (57)$$

The incident field (53) has only x and y components. So that only the xx, xy, yx and yy components of the conductivity tensor are involved in the conduction process driven by field (53). In consonance with Eq.(56), one should make the substitution

$$v_{BA}^x \to v_{\parallel}^{BA}\sin\theta\cos\phi, \;\; v_{BA}^y \to v_{\parallel}^{BA}\sin\theta\sin\phi, \quad (58)$$

in the conductivity tensor (1). The angular part of integral (57) can be carried out. From Eqs.(57,58), one can see $\sigma_{xy} = \sigma_{yx} = 0$ and $\sigma_{xx} = \sigma_{yy} = \sigma$. Because the factors in Eq.(1) do not depend on the position of localized state ϕ_A, one can carry out the spatial integral in $\sum_A$. The conductivity from LE transitions is

$$\begin{cases} \text{Re} \\ \text{Im} \end{cases} \sigma(\omega) = \frac{4\pi\overline{\xi}^3}{3}\frac{bZe^2 n_{loc}}{4\pi\epsilon_0\varepsilon U}\frac{8ne^2}{3\pi\hbar^3 m^2}\int_0^{\infty} d\xi \int_0^{\infty} dp$$

$$\times[1 - f(E_{B_1})]f(E_A)\frac{p^4}{(E_{B_1}^0 - E_A^0)}\frac{\xi\exp(-\frac{bZe^2}{4\pi\epsilon_0\varepsilon U\xi})}{(1 + p^2\xi^2/\hbar^2)^4} \quad (59)$$

$$\times\frac{\sqrt{\pi}\hbar}{2(k_BT\lambda_{BA})^{1/2}}[e^{-\frac{\lambda_{BA}}{4k_BT}(1+\frac{\hbar\omega_{BA}-\hbar\omega}{\lambda_{BA}})^2} \pm e^{-\frac{\lambda_{BA}}{4k_BT}(1+\frac{\hbar\omega_{BA}+\hbar\omega}{\lambda_{BA}})^2}],$$

where $n = N_e/\Omega_{\mathbf{s}}$ is the carrier concentration, E_A and E_{B_1} are given in Eqs.(15,20). From Eq.(59), one can easily compute TCR: $\rho^{-1}\frac{d\rho}{dT} = -\sigma^{-1}\frac{d\sigma}{dT}$, an important material parameter for bolometer[1,55]. σ and TCR are expressed with easy access quantities: U and E_c for localized states, ε and q_{TF} for the interaction between electron and atomic core, the averaged sound speed $\overline{c}$ for the vibrations.

B. EL transitions driven by external field

Since the field-matter coupling is Hermitian, the corresponding expressions for EL transition driven by field can be obtained from those for LE transitions driven by field through exchanging the status of ϕ_A and χ_B.

$$\begin{cases} \text{Re} \\ \text{Im} \end{cases} \sigma(\omega) = \frac{4\pi\overline{\xi}^3}{3}\frac{bZe^2 n_{loc}}{4\pi\epsilon_0\varepsilon U}\frac{8ne^2}{3\pi\hbar^3 m^2}\int_0^{\infty} d\xi \int_0^{\infty} dp$$

$$\times[1 - f(E_A)]f(E_B)\frac{p^4}{(E_A^0 - E_B^0)}\frac{\xi\exp(-\frac{bZe^2}{4\pi\epsilon_0\varepsilon U\xi})}{(1 + p^2\xi^2/\hbar^2)^4} \quad (60)$$

$$\times\frac{\sqrt{\pi}\hbar}{2(k_BT\lambda_{AB})^{1/2}}[e^{-\frac{\lambda_{AB}}{4k_BT}(1+\frac{\hbar\omega_{AB}-\hbar\omega}{\lambda_{AB}})^2} \pm e^{-\frac{\lambda_{AB}}{4k_BT}(1+\frac{\hbar\omega_{AB}+\hbar\omega}{\lambda_{AB}})^2}],$$

where

$$y_{\pm}^{AB} = \frac{(\omega_{BA} \pm \omega)^2}{4\lambda_{AB}k_BT}, \quad \lambda_{AB} = \frac{1}{2}\sum_{\alpha}\hbar\omega_{\alpha}(\theta_{\alpha}^A)^2. \quad (61)$$

For the LE transition driven by the transfer integral and the EL transition driven by e-ph interaction, one does not have this symmetry[6,7].

C. LL transition driven by external field

One can similarly find the conductivity from the LL transitions driven by external field (Fig.2a of [7]):

$$\begin{cases} \text{Re} \\ \text{Im} \end{cases} \sigma_{\alpha\beta}(\omega) = -\frac{N_e e^2}{2\Omega_s}\sum_{AA_1}\text{Im}\frac{(w_{AA_1}^{\alpha} - v_{A_1A}^{\alpha})(v_{A_1A}^{\beta})^*}{(E_A^0 - E_{A_1}^0)}$$

$$\times i[I_{A_1A+} \pm I_{A_1A-}][1 - f(E_{A_1})]f(E_A), \quad (62)$$

where the velocity matrix elements are

$$w_{AA_1}^{\alpha} = -\frac{i\hbar}{m}\int d^3x\phi(\mathbf{r} - \mathbf{R}_A)\frac{\partial}{\partial x_{\alpha}}\phi^*(\mathbf{r} - \mathbf{R}_{A_1}), \quad (63)$$

and

$$v_{A_1A}^{\alpha} = -\frac{i\hbar}{m}\int d^3x\phi^*(\mathbf{r} - \mathbf{R}_{A_1})\frac{\partial}{\partial x_{\alpha}}\phi(\mathbf{r} - \mathbf{R}_A). \quad (64)$$

$v_{A_1A}^{\alpha}$ is given in Eq.(A2) and $w_{AA_1}^{\alpha} = -v_{A_1A}^{\alpha}$. The time integral

$$I_{A_1A\pm}(\omega) = \exp\{-\frac{1}{2}\sum_{\alpha}(\theta_{\alpha}^{A_1} - \theta_{\alpha}^A)^2\coth\frac{\beta\hbar\omega_{\alpha}}{2}\} \quad (65)$$

$$\times\int_{-\infty}^{0} ds e^{\pm i\omega s}e^{-is(E'_{A_1} - E'_A)/\hbar}\times$$

$$\exp[\frac{1}{2}\sum_{\alpha}\frac{(\theta_{\alpha}^{A_1}-\theta_{\alpha}^{A})^2}{2}(\coth\frac{\beta\hbar\omega_{\alpha}}{2}\cos\omega_{\alpha}s+i\sin\omega_{\alpha}s)],$$

contains the primary temperature dependence of conductivity. At high temperature $k_BT \geq \hbar\overline{\omega}$, $I_{A_1A\pm}$ reduces to

$$I_{A_1A\pm}(\omega) = -i\hbar/\lambda_{A_1A} \tag{66}$$

$$+\frac{\hbar e^{-\beta\hbar(\pm\omega+\omega_{AA_1})/2-y_{\pm}^{A_1A}-\beta\lambda_{A_1A}/4}}{(\lambda_{A_1A}k_BT)^{1/2}}[\frac{\sqrt{\pi}}{2}-iA(y_{\pm}^{A_1A})],$$

where

$$\lambda_{A_1A} = \frac{1}{2}\sum_{\alpha}\hbar\omega_{\alpha}(\theta_{\alpha}^{A_1}-\theta_{\alpha}^{A})^2, \tag{67}$$

and

$$y_{\pm}^{A_1A} = \frac{[\hbar(\pm\omega+\omega_{AA_1})]^2}{4\lambda_{A_1A}k_BT}. \tag{68}$$

To carry out the summation over initial and final electronic states, we first fix the initial electronic state A. We take the center $\mathbf{R}_A$ of localized state $\phi_A(\mathbf{r}-\mathbf{R}_A)$ as the origin, the incident direction $\mathbf{k}$ of the electromagnetic wave as the polar axis. Denote $R = R_{AA_1} = |\mathbf{R}_{A_1}-\mathbf{R}_A|$ the distance between the centers of localized states $\phi_{A_1}(\mathbf{r}-\mathbf{R}_{A_1})$ and ϕ_A, the unit vector along $(\mathbf{R}_{A_1}-\mathbf{R}_A)$ is $\mathbf{n}_{AA_1} = (X_{AA_1}, Y_{AA_1}, Z_{AA_1})/R_{AA_1}$, where $(X_{AA_1}, Y_{AA_1}, Z_{AA_1})$ are the Cartesian components of vector $\mathbf{R}_{A_1}-\mathbf{R}_A$.

Since the conductivity tensor is usually expressed in a system of Cartesian coordinates, we introduce an auxiliary Cartesian system $(\boldsymbol{\epsilon}_1, \boldsymbol{\epsilon}_2, \mathbf{k})$, where $\boldsymbol{\epsilon}_1$ and $\boldsymbol{\epsilon}_2$ are the two linear polarization vectors. The electric field $\mathbf{F}$ has only x and y components: $\mathbf{F} = F_1\boldsymbol{\epsilon}_1 + F_2\boldsymbol{\epsilon}_2 + 0\mathbf{k}$. Because we sum over A_1, the centers $\mathbf{R}_{A_1}$ of localized states $\phi_{A_1}(\mathbf{r}-\mathbf{R}_{A_1})$ sit at different points. To simplify the calculation of the velocity matrix elements, we resolve the position vector $\mathbf{r}$ of electron in an orthogonal frame:

$$\mathbf{r} = r_{\perp 1}\mathbf{l}_{AA_1} + r_{\perp 2}\mathbf{m}_{AA_1} + r_{\parallel}\mathbf{n}_{AA_1}, \tag{69}$$

where $\mathbf{l}_{AA_1}$ and $\mathbf{m}_{AA_1}$ are two unit vectors perpendicular to each other and to $\mathbf{n}_{AA_1}$. From Eq.(A4), one has

$$\langle\phi_{A_1}|\mathbf{r}|\phi_A\rangle = \mathbf{n}_{AA_1}\langle\phi_{A_1}|r_{\parallel}|\phi_A\rangle. \tag{70}$$

By means of Eq.(70), the perturbation of the electric field is

$$\langle\phi_{A_1}|\mathbf{F}\cdot\mathbf{r}|\phi_A\rangle = \mathbf{F}\cdot\mathbf{n}_{AA_1}\langle\phi_{A_1}|r_{\parallel}|\phi_A\rangle \tag{71}$$

$$= \sin\theta(F_1\cos\phi + F_2\sin\phi)\frac{i\hbar v_{\parallel}^{A_1A}}{(E_A-E_{A_1})},$$

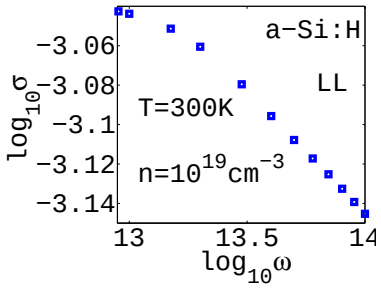

(a)

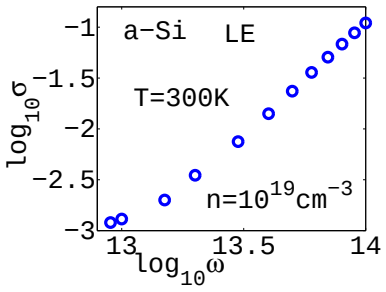

(b)

FIG. 7: Conductivity as function of frequency at T=300K. 7(a): LL transition; 7(b):LE transition. In the frequency range, the contribution from LE transition is more important than that from LL transitions.

where $v_{\parallel}^{A_1A}$ has been obtained in appendix A. The angular integrals in summation $\sum_{A_1}$ can be effected: $\sigma_{xy} = \sigma_{yx} = 0$ and $\sigma_{xx} = \sigma_{yy} = \sigma$. Because of the uniformity of AS, the spatial integral in $\sum_A$ can be carried out. The conductivity from LL transition driven by field is

$$\begin{cases}\text{Re}\\ \text{Im}\end{cases}\ \sigma(\omega) = \frac{4\pi\overline{\xi}^3}{3}[\frac{bZe^2n_{loc}}{4\pi\epsilon_0\varepsilon U}]^2\int_0^{\infty}\frac{d\xi_1}{\xi_1^2}\exp(-\frac{bZe^2}{4\pi\epsilon_0\varepsilon U\xi_1})$$

$$\times\int_0^{\infty}\frac{d\xi_2}{\xi_2^2}\exp(-\frac{bZe^2}{4\pi\epsilon_0\varepsilon U\xi_2})ne^2\frac{[1-f(E_{A_1})]f(E_A)}{2(E_A^0-E_{A_1}^0)}$$

$$\times\frac{\sqrt{\pi}\hbar}{2(\lambda_{A_1A}k_BT)^{1/2}}[e^{-\frac{\lambda_{A_1A}}{4k_BT}(1+\frac{\hbar\omega_{A_1A}-\hbar\omega}{\lambda_{A_1A}})^2}\pm e^{-\frac{\lambda_{A_1A}}{4k_BT}(1+\frac{\hbar\omega_{A_1A}+\hbar\omega}{\lambda_{A_1A}})^2}]$$

$$\times\int_0^{R_c}R^2dR\frac{4\pi}{3}(w_{\parallel}^{AA_1}-v_{\parallel}^{A_1A})(v_{\parallel}^{A_1A})^*, \tag{72}$$

where and in appendix, to shorten the symbols, we use ξ_2 instead of ξ_{A_1}, use ξ_1 instead of ξ_A.

We can see from Eqs.(59,60,72) that when $\omega = 0$, $\text{Im}\,\sigma = 0$ for LL, LE and EL transitions. For two n-doped a-Ge:H samples with $n = 10^{18}$ and 10^{19}cm^{-3}, $\log_{10}\sigma$ and TCR from LL, LE and EL transitions as functions of temperature at $\omega = 0$ are plotted in Fig.4. The corresponding results at $\omega = 10^{13}$ Hz are plotted in Fig.

5. Re σ increases with frequency while TCR decreases with frequency. For two n-doped a-Si:H samples, the conductivity and TCR as functions of temperature at $\omega = 10^{13}$Hz are plotted in Fig.6, the results at $\omega = 0$ was reported in [54]. The calculated TCR for a-Si:H falls[54] in the observed[55,57,58] range between -2% and -8%.

At $\omega = 0$, the conductivity from LE transition is the same order of magnitude as that from LL transitions, the conductivity from EL transitions is much smaller than those from LL and LE transitions. There is a crossover temperature T*, below T* the conductivity from LL transitions is larger than the conductivity from LE transitions, above T* the conductivity from LE transitions is larger. Because the activation energy for LL transitions is different to that for LE transitions, this phenomenon explained the kink on the observed $\log_{10}\sigma$ vs. 1/T curve[54].

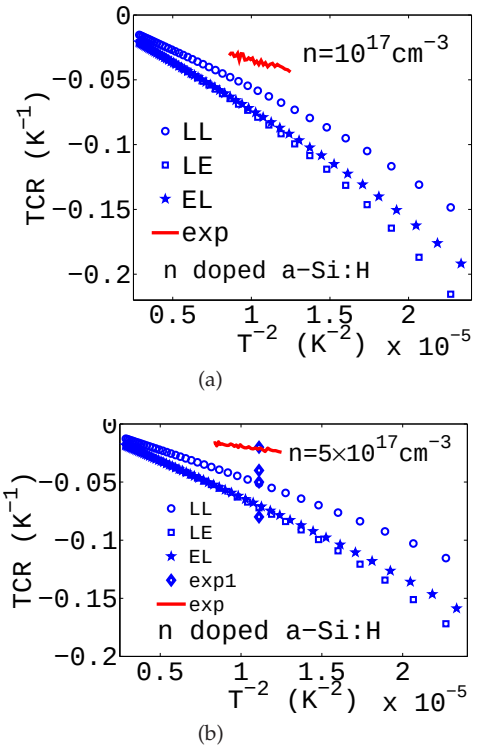

FIG. 8: (color online) TCR as function of temperature in two n-doped a-Si:H with $n = 10^{17}cm^{-3}$ and $5 \times 10^{17}cm^{-3}$, the diamond symbol data are taken from [47,48], the solid line experimental data taken from [56].

For two n-doped a-Si:H samples at 300K, $\log_{10}\sigma(\omega)$ vs. $\log_{10}\omega$ in a frequency range 10^{13} to 10^{14}Hz is illustrated in Fig. 7(b). We can see that (i) the conductivity of LL transitions slowly decreases with ω; (ii) the conductivity from LE transitions increases rapidly with frequency. The total conductivity is a sum from various processes[7], and the conductivity from LL transitions is smaller than that from the LE transitions at higher frequency. The total conductivity arises mainly from LE transitions at higher frequencies. The general trend in $\log_{10}\sigma(\omega)$ vs. $\log_{10}\omega$ is not far from Tanaka and Fan's[59] result $\sigma(\omega) \sim \omega^2$, but obviously deviates from the simple power law around 10^{13}Hz. We must be cautious that the results derived in this work is only suitable to the contributions from electrons: at such high frequency the ionic contribution should also be included.

In Fig.8, we compared the observed and calculated TCR for two n-doped a-Si:H with $n = 10^{17}cm^{-3}$ and $5 \times 10^{17}cm^{-3}$. The calculations roughly agree with the experiment[56] in temperature range 282K-349K. The observed absolute values of TCR is systematically smaller than those of calculated. This is due to the samples contain micro-crystalline grains in the amorphous matrix[55], while crystalline material has smaller absolute value of TCR. Fig.9 is the comparisons for conductivity.

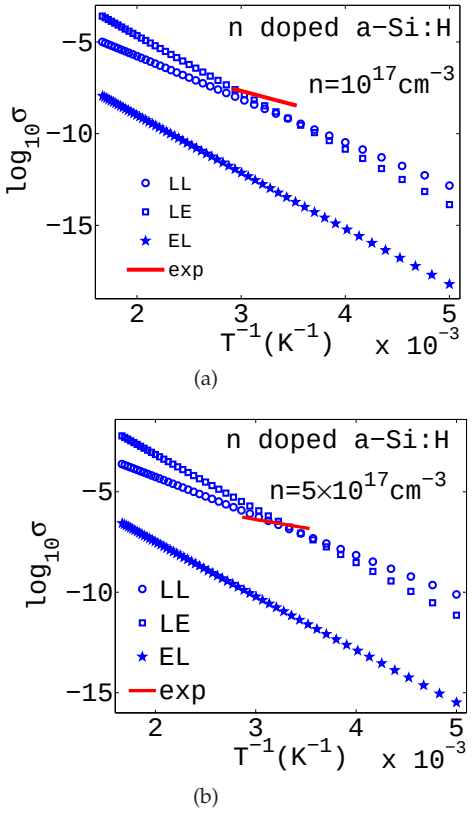

FIG. 9: (color online) DC conductivity as function of temperature in two n-doped a-Si:H with $n = 10^{17}cm^{-3}$ and $5 \times 10^{17}cm^{-3}$, experimental data taken from [56].

IV. CONCLUSION

The microscopic response method expresses transport coefficients with transition amplitude rather than transition probability per unit time, and may be used in amorphous semiconductors in which Landau-Peierls condition is violated[3,4].

We presented an approximate theory for the conductivity and Hall mobility in amorphous semiconductors systematically derived from the MRM. We obtained the temperature dependence of the conductivity from the three simplest transitions: LL, LE and EL transitions driven solely by field, cf. Eqs.(62,59,60). The conductivity is expressed in terms of accessible physical quantities: mobility edge, Urbach energy, static dielectric constant and elastic modulus. LE transition (ignored in previous theories) contributes to conductivity in the same order as LL and EE transitions. Below a crossover temperature T*, the conductivity from LL transitions is larger than that from LE transitions; above T, the conductivity form LE transitions is larger. This phenomenon, and different activation energy for LL and LE transitions is the reason for the kink in the observed conductivity vs. 1/T curve. We show how a kinetic theory of transport can be properly generalized for AS.

Acknowledgments

We would like to express our deep appreciation to Drs. D. B. Saint John and N. J. Podraza giving us their unpublished resistivity vs. temperature raw data[56] of n-doped a-Si:H samples, which made a broader comparison with experiments possible. We thank for support from the U.S. Army Research Laboratory and the U. S. Army Research Office under grant number W911NF-11-1-0358 and NSF under DMR 09-03225 .

Appendix A: velocity matrix elements between two localized states

To calculate the velocity matrix elements in Eq.(64), it is convenient to adopt a system of spherical coordinates. We take the center $\mathbf{R}_A$ of localized state $\phi_A(\mathbf{r}-\mathbf{R}_A)$ as the origin $\mathbf{R}_A = 0$, the connection line $\mathbf{R}_{A_1}-\mathbf{R}_A$ between the centers of two localized states as the polar axis. Denote $r = |\mathbf{r}-\mathbf{R}_A|$ and $r_2 = |\mathbf{r}-\mathbf{R}_{A_1}| = [r^2+R^2-2rR\cos\theta]^{1/2}$, where $R = \mathbf{R}_{A_1}-\mathbf{R}_A$, θ is the angle between $\mathbf{r}-\mathbf{R}_A$ and $\mathbf{R}_{A_1}-\mathbf{R}_A$. The v_z matrix element can be written as

$$v^z_{A_1A} = -\frac{i\hbar}{m}\pi^{-1}\xi_1^{-3/2}\xi_2^{-3/2}\int_0^\infty r^2dr$$

$$\int_0^\pi \sin\theta d\theta\int_0^{2\pi} d\phi e^{-r_2/\xi_2}\frac{\partial}{\partial z}e^{-r/\xi_1},$$

and one has similar expressions for the matrix elements of v_x and v_y. Because r_2 does not depend on the azimuth angle ϕ,

$$v^x_{A_1A} = v^y_{A_1A} = 0. \tag{A1}$$

We condense them as $v_\perp^{A_1A} = 0$: the matrix element for any component of velocity perpendicular to the connection line between two localized states is zero.

The ϕ integral is immediate, the remaining r and θ integrals in $v^z_{A_1A}$ can be calculated by changing the integration variable θ to r_2 for a fixed r. With the help of $\cos\theta = \frac{r^2+R^2-r_2^2}{2rR}$ and $\sin\theta d\theta = \frac{r_2dr_2}{Rr}$, the integral over θ becomes an integral over r_2. One first carries out the integral over r_2, then carries out the integral over r. For the velocity component parallel to the connection line between two localized states, the matrix element is

$$v_\parallel^{A_1A} = -\frac{i\hbar}{m}\pi^{-1}\xi_1^{-3/2}\xi_2^{-3/2}\int d^3x e^{-r_2/\xi_2}\nabla_\parallel e^{-r/\xi_1}$$

$$= -\frac{i\hbar}{m}(\xi_1\xi_2)^{-3/2}\{-4(\frac{\xi_2^2}{R^2}+\frac{\xi_2}{R})\frac{e^{-R/\xi_2}\xi'^3}{\xi_1}$$

$$-(2+6\frac{\xi_2}{R}+6\frac{\xi_2^2}{R^2})\frac{\xi_2 e^{-R/\xi_2}\xi'^2}{\xi_1}-(2+6\frac{\xi_2}{R}+6\frac{\xi_2^2}{R^2})\frac{\xi_2^2e^{-R/\xi_2}\xi'}{\xi_1}$$

$$+(\frac{2}{\xi_2R}+\frac{2}{R^2})\frac{\xi_2^2e^{-R/\xi_2}\xi''^3}{\xi_1}[2-(R^2/\xi''^2+2R/\xi''+2)e^{-R/\xi''}]$$

$$-(\frac{2}{\xi_2}+\frac{6}{R}+6\frac{\xi_2}{R^2})\frac{\xi_2^2e^{-R/\xi_2}\xi''^2}{\xi_1}[1-(R/\xi''+1)e^{-R/\xi''}]$$

$$+(2+6\frac{\xi_2}{R}+6\frac{\xi_2^2}{R^2})\frac{\xi_2^2e^{-R/\xi_2}\xi''}{\xi_1}(1-e^{-R/\xi''})$$

$$+(\frac{2}{R^2}-\frac{2}{R\xi_2})\frac{\xi_2^2e^{-R/\xi_1}\xi'^3}{\xi_1}(\frac{R^2}{\xi'^2}+2\frac{R}{\xi'}+2)$$

$$+(\frac{6\xi_2}{R^2}+\frac{2}{\xi_2}-\frac{6}{R})\frac{\xi_2^2e^{-R/\xi_1}\xi'^2}{\xi_1}(\frac{R}{\xi'}+1)$$

$$+(2-6\frac{\xi_2}{R}+6\frac{\xi_2^2}{R^2})\frac{\xi_2^2e^{-R/\xi_1}\xi'}{\xi_1}\}, \tag{A2}$$

where ξ' and ξ'' are defined by

$$\xi'^{-1} = \xi_1^{-1}+\xi_2^{-1} \text{ and } \xi''^{-1} = \xi_1^{-1}-\xi_2^{-1}.$$

Eq.(A2) displays the exponential decay of velocity matrix elements with distance R between two localized states. In the variable range hopping argument[2], only the exponential decay of transfer integral with R is treated. In a process which is first order in transfer integral, that is not discussed here, one may expect interesting new features.

Because for each Cartesian component,

$$\langle \phi_{A_1} | x_\alpha | \phi_A \rangle = \frac{i\hbar \langle \phi_{A_1} | v_\alpha | \phi_A \rangle}{(E_A - E_{A_1})}, \quad \alpha = x, y, z, \qquad \text{(A3)}$$

from (A1) and (A2), one has

$$\langle \phi_{A_1} | r_\perp | \phi_A \rangle = 0 \text{ and } \langle \phi_{A_1} | r_\parallel | \phi_A \rangle = \frac{i\hbar v_\parallel^{A_1 A}}{(E_A - E_{A_1})}. \qquad \text{(A4)}$$

[1] R. A. Street, *Hydrogenated Amorphous Silicon*, Cambridge Univresity Press, Cambridge (1991).

[2] N. F. Mott and E. A. Davis, *Electronic Processes in Non-crystalline Materials*, Clarendon Press, Oxford, (1971).

[3] R. Peierls, *Surprises in Theoretical Physics*, pp121-126, Princeton University Press, Princeton (1979).

[4] R. Peierls, *Qunatum Theory of Solids*, pp139-142, Clarendon Press, Oxford (1955).

[5] E. M. Lifshitz and L. P. Pitaevskii, *Physical Kinetics*, Butterworth-Heinemann, Oxford (1981).

[6] M.-L. Zhang and D. A. Drabold, Eur. Phys. J. B. **77**, 7-23, (2010).

[7] M.-L. Zhang and D. A. Drabold, Phys. Status Solidi B **248**, 2015-2026, (2011).

[8] A. Miller and E. Abrahams, Phys. Rev. **120**, 745 (1960).

[9] H. Overhof and P. Thomas, *Electronic Transport in Hydrogenated Amorphous Semiconductor*, Springer-Verlag, Berlin (1989).

[10] M.-L. Zhang and D. A. Drabold, Phys. Rev. Lett. **105**, 186602 (2010).

[11] M.-L. Zhang and D.A. Drabold, Phys. Rev. B**81**, 085210 (2010).

[12] P.G. Le Comber and J. Mort, *Electronic and Structural Properties of Amorpous Semiconductors*, Academic Press, London, (1973).

[13] W. H. Butler, Phys. Rev. B**31**, 3260, (1985).

[14] J. Banhart, Phys. Rev. Lett. 82, 2139, (1999).

[15] G. D. Mahan, *Many-Particle Physics*, Second edition, Plenum Press, New York (1990).

[16] W. Beyer and H. Mell, in *Amorphous and Liquid Semiconductors*, p.333, ed. by W. E. Spear, CICL, Edinburgh (1977).

[17] M. Cliffe, M. T. Dove, D. A. Drabold and A. L. Goodwin, Phys. Rev. Lett. **104**, 125501 (2010).

[18] L. D. Landau and E. M. Lifshitz, *Theory of Elasticity*, Third edition, Butterworth-Heinemann, London (1986).

[19] N. W. Ashcroft and N. D. Mermin, *Solid State Physics*, Holt, Rinehart and Winston, NewYork (1976).

[20] W. A. Kamitakahara, C. M. Soukoulis and H. R. Shanks, U. Buchenau and G. S. Grest, Phys. Rev. B **36**, 6539 (1987).

[21] L. D. Landau and E. M. Lifshitz, *Mechanics*, Third edition, Butterworth-Heinemann, London (1976).

[22] N. F. Mott, *Conduction in Non-Crystalline Materials*, Second edition, Clarendon Press, Oxford (1993).

[23] Y. Pan, M. Zhang and D. A. Drabold, J. Non. Cryst. Sol. **354**, 3480 (2008).

[24] Y. Pan, F. Inam, M. Zhang and D. A. Drabold, Phys. Rev. Lett. **100**, 206403 (2008).

[25] D. A. Drabold, Y. Li, B. Cai and M.-L. Zhang, Phys. Rev. B **83**, 045201 (2011).

[26] J. J. Ludlam, S. N. Taraskin, S. R. Elliott and D. A. Drabold, J. Phys. Cond. Matter **17**, L321 (2005).

[27] F. Inam, J. P. Lewis and D. A. Drabold, Phys. Stat. Sol. A**207**, 599 (2010).

[28] J. H. Davis, J. Non-Cryst. Solids **35**, 67-69 (1980).

[29] F. Orapunt and S. K. O'Leary, J. Appl. Phys. **104**, 073513 (2008).

[30] J. Dong and D. A. Drabold, Phys. Rev. Lett. **80**, 1928 (1998).

[31] R. B. Wehrspohn, S. C. Deane, I. D. French, I. G. Gale, M. J. Powell and R. Brüggemann, Applied Physics Letters **74**, 3374 (1999).

[32] taken from Y.-T. Li and D.A. Drabold's unpublished calculation.

[33] F. Urbach, Phys. Rev. **92**, 1324 (1953).

[34] S. Aljishi, J. D. Cohen, S. Jin and L. Key, Phys. Rev. Letter **64**, 2811 (1990).

[35] Y. Kanemitsu, M. Iiboshi and T. Kushida, Apply. Phys. Lett. **76**, 2200 (2000).

[36] M. Ivanda, Phys. Rev. B**46**, 14893 (1992).

[37] Q. Gu, E.A. Schiff, J. Chevrier and B. Equer, Phys. Rev. B**52**, 5695 (1995).

[38] M. Stutzmann and J. Stuke, Solid State Communications, **47**, 635-639 (1983).

[39] I. Yassievich, M. Bresler and O. Gusev, J. Non-Cryst. Solids **226**, 192-199 (1998).

[40] J. A. Howard asnd R. A. Street, Phys. Rev. B**44**, 7935 (1991).

[41] E. Louis and J. A. Verges, Solid State Communications, **60**, 157-160 (1986).

[42] B. Velicky, Phys. Rev. **184**, 614 (1969).

[43] M.-L. Zhang and D.A. Drabold, Phys. Rev. B**78**, 195208 (2008).

[44] T. Holstein, Ann. Phys. **8**, 325 (1959); 343 (1959).

[45] D. A. Drabold, P. A. Fedders, S. Klemm and O. F. Sankey, Phys. Rev. Lett., **67**, 2179 (1991).

[46] R. Atta-Fynn, P. Biswas and D. A. Drabold, Phys. Rev. B **69**, 245204 (2004).

[47] A. Torres, A. Kosarev, M.L. Garcia Cruz , R. Ambrosio, Journal of Non-Crystalline Solids **329**, 179–183 (2003).

[48] A. Inoue, M. Yamamoto, H. M. Kimura and T. Masumoto, Journal of Materials Science Letters **6**,194-196 (1987).

[49] D. A. Greenwood, Proc.Phys.Soc. **71**, 585-596 (1958).

[50] C. M. Bender and S. A. Orszag, *Advanced Mathematical Methods For Sciencetists and Engineers*, McGraw-Hill, New York (1978).

[51] S. K. Bahl and N. Bluzer, in Tetradrally Bonded Amorpous

Semiconductors, p320, edited by M. H. Brodsky, S. Kirkpatric and D. Weaire, AIP, NewYork (1974).
[52] M. H. Brodsky and A. Lurio, Phys. Rev. B**9**, 1646 (1974).
[53] M. C. Payne, A. F. J. Levit, W. A. Phillips, J. C. Inkson and C J Adkins, J. Phys. C: Solid State Phys. **17**, 1643 (1984).
[54] M.-L. Zhang and D.A. Drabold, arXiv:1112.2169v2, Europhys. Lett., accepted.
[55] D. B. Saint John, H.-B. Shin, M.-Y. Lee, S. K. Ajmera, A. J. Syllaios, E. C. Dickey, T. N. Jackson, and N. J. Podraza, J. Appl. Phys. **110**, 033714 (2011).
[56] D. B. Saint John, H.-B. Shin, M.-Y. Lee, S. K. Ajmera, A. J. Syllaios, E. C. Dickey, T. N. Jackson, and N. J. Podraza, unpublished resistivity vs. temperature raw data.
[57] A. Orduna-Diaza, C.G. Trevino-Palaciosa, M. Rojas-Lopezb, R. Delgado-Macuilb, V.L. Gayoub, A. Torres-Jacomea, Materials Science and Engineering B **174**, 93–96 (2010).
[58] P. W. Kruse, *Uncooled thermal imaging: arrays, systems, and applications*, SPIE Press, (2001).
[59] S. Tanaka and H. Y. Fan, Phys. Rev. **132**, 1516 (1963).